

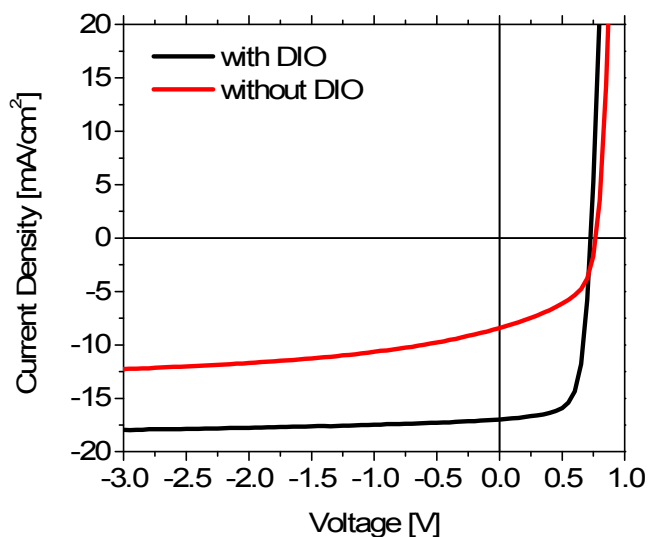
# The Effect of Solvent Additive on Generation, Recombination and Extraction in PTB7:PCBM Solar Cells: A Conclusive Experimental and Numerical Simulation Study

*Juliane Kniepert, Ilja Lange, Jan Heidbrink, Jona Kurpiers, Thomas J. K. Brenner, L. Jan Anton Koster<sup>†</sup>, and Dieter Neher\**

Institute of Physics and Astronomy, University of Potsdam  
Karl-Liebknecht-Str. 24-25, 14476, Potsdam, Germany

Supporting Information

(a)



(b)

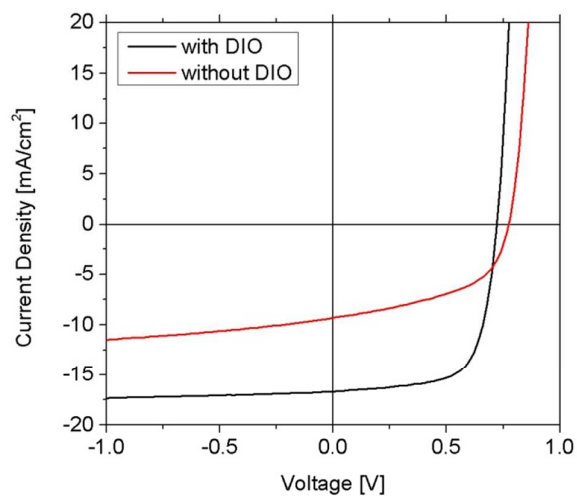


**Figure S1.** (a)  $J$ - $V$  characteristics for the PTB7:PCBM devices processed with (black line) and without (red line) DIO. At high reverse bias the photocurrent saturates at  $17.6 \text{ mA/cm}^2$  (with DIO) and  $12.5 \text{ mA/cm}^2$  (without DIO). These values were used to calculate the generation rates with equation 1. (b)  $J$ - $V$  characteristics of the second PTB7 batch, used to perform the wavelength dependent TDCF studies from Figure 2b (main text).

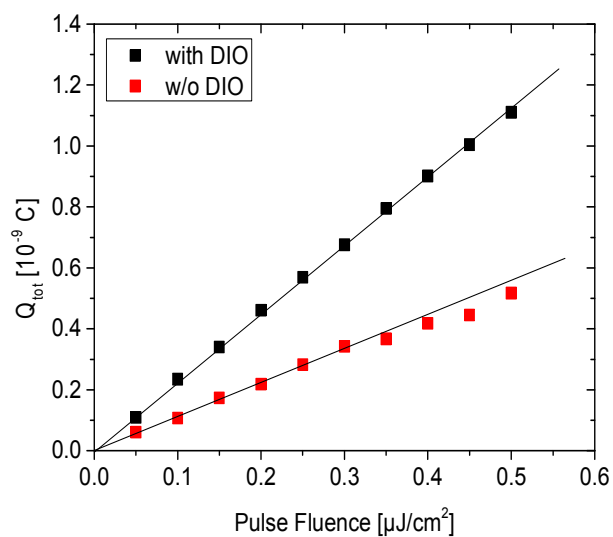


**Figure S2.** Total extracted charge ( $Q_{\text{tot}}$ ) determined with TDCF as a function of laser pulse fluence. The lines are guides to the eye. The strict linear dependence of  $Q_{\text{tot}}$  on excitation density proves that non-geminate recombination is insignificant under the applied conditions.  $V_{\text{coll}}$  was  $-2.5 \text{ V}$  and  $V_{\text{pre}}$  was  $0.7 \text{ V}$ .

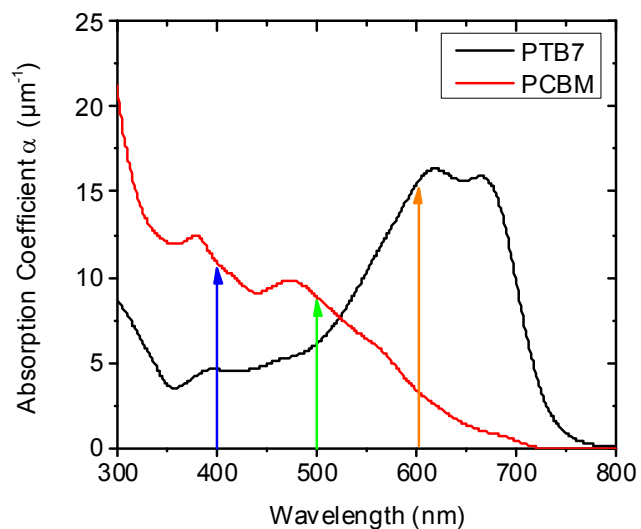


**Figure S3.** Absorption spectra of pristine PTB7 (black line) and pristine PC<sub>70</sub>BM (red line). The coloured arrows indicate the different excitation wavelengths that were used for Figure 2b (blue – 405 nm, green – 500 nm, orange – 600 nm). At 405 nm PCBM is predominantly excited whereas at 600 nm PTB7 is predominantly excited.

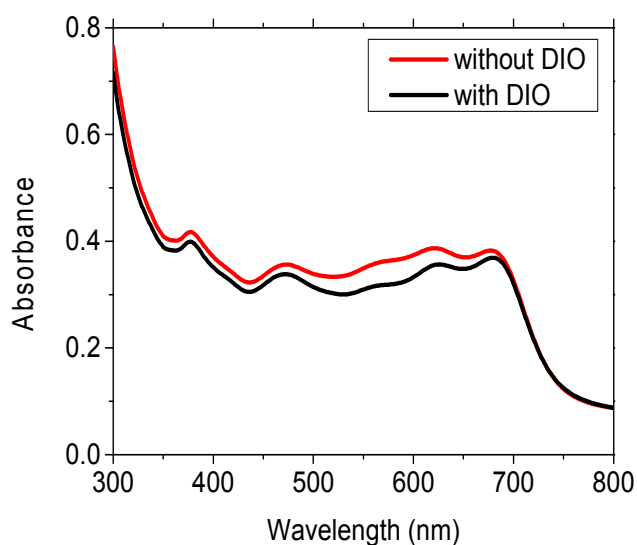


**Figure S4.** Absorption spectra of PTB7:PCBM blend processed with (black line) and without (red line) DIO.

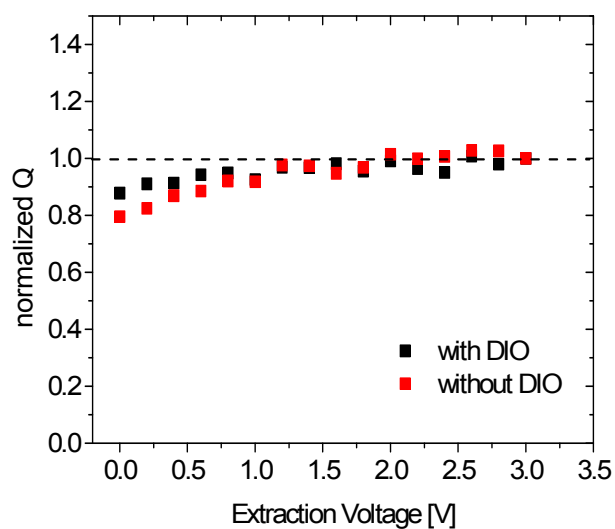


**Figure S5.** Extracted charge determined with BACE as a function of extraction voltage. Without external bias only 80% of the charge is extracted in the blend without DIO and 90% of the charge is extracted in the blend with DIO. For both blends  $V_{\text{ext}} = 2.5$  V is sufficient to extract all photogenerated charge carriers.

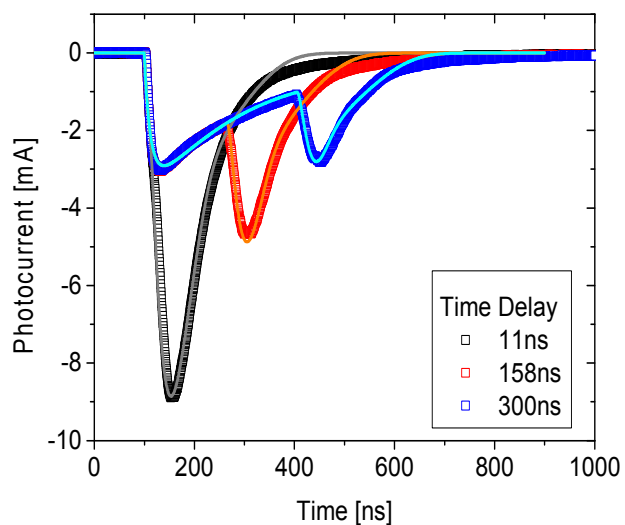


**Figure S6.** TDCF transients of the devices with DIO – measured data (symbols) and fit with a numerical transient drift-diffusion simulation (solid lines). The time delay between laser pulse and extraction pulse was 11 ns (black), 158 ns (red) and 300 ns. The input parameters for the simulation are summarized in Table S1.

initial carrier density	$6.5 \times 10^{22} \text{ m}^{-3}$
electron mobility	$3 \times 10^{-4} \text{ cm}^2 \text{ V}^{-1} \text{ s}^{-1}$
Poole-Frenkel factor for electrons	$-0.001 \text{ cm}^{1/2} \text{ V}^{-1/2}$
hole mobility	$4.5 \times 10^{-4} \text{ cm}^2 \text{ V}^{-1} \text{ s}^{-1}$
Poole-Frenkel factor for holes	0
bimolecular recombination coefficient	$1.6 \times 10^{-17} \text{ m}^3 \text{ s}^{-1}$

**Table S1.** Parameters used for the transient drift-diffusion simulation of the PTB7:PCBM devices prepared with DIO in Figure S6.

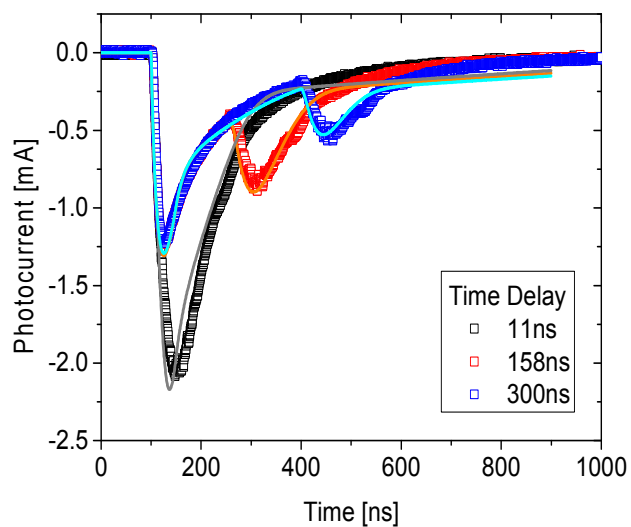


**Figure S7.** TDCF transients of the devices without DIO – measured data (symbols) and fit with a numerical transient drift-diffusion simulation (solid lines). The time delay between laser pulse and extraction pulse was 11 ns (black), 158 ns (red) and 300 ns. The input parameters for the simulation are summarized in Table S2.

initial carrier density	$2.5 \times 10^{22} \text{ m}^{-3}$
electron mobility	$3 \times 10^{-5} \text{ cm}^2 \text{ V}^{-1} \text{ s}^{-1}$
Poole-Frenkel factor for electrons	0
hole mobility	$9 \times 10^{-4} \text{ cm}^2 \text{ V}^{-1} \text{ s}^{-1}$
Poole-Frenkel factor for holes	$-0.003 \text{ cm}^{1/2} \text{ V}^{-1/2}$
bimolecular recombination coefficient	$5 \times 10^{-17} \text{ m}^3 \text{ s}^{-1}$

**Table S2.** Parameters used for the transient drift-diffusion simulation of the PTB7:PCBM devices prepared without DIO in Figure S7.

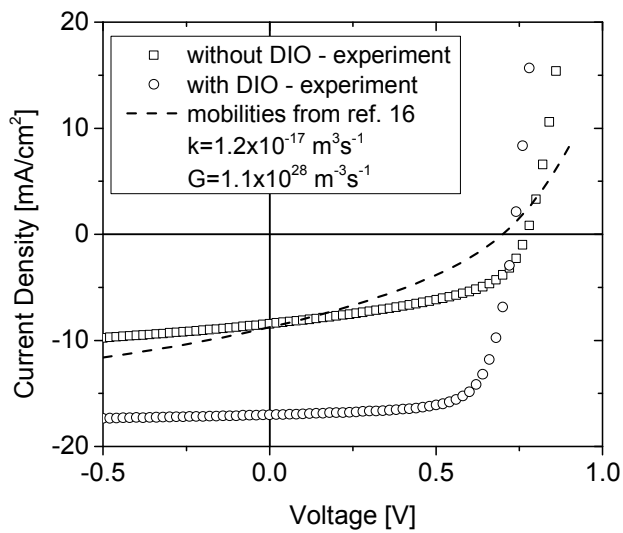


**Figure S8.** Dashed line: Numerical simulation using the charge carrier mobilities determined in reference [16] for the device with DIO, i.e.  $\mu_n=1.5 \times 10^{-4} \text{ cm}^2/\text{Vs}$  and  $\mu_e=1.5 \times 10^{-5} \text{ cm}^2/\text{Vs}$ , and the generation and recombination rates as reliably determined in our measurements. Symbols: Measured  $I$ - $V$  characteristics.

## Determination of the band gap

In order to determine the effective band gap between PTB7-HOMO and PCBM-LUMO, two different techniques have been applied. In the first method, the  $V_{OC}$  of the devices at multiple illumination intensities is analyzed as a function of the carrier density  $n$  using the fundamental approach

$$V_{OC} = E_g + 2k_B T * \ln\left(\frac{n}{N}\right)$$

(see Ref. Lange et al., *J. Phys. Chem. Lett.* (2013), 4, 3865). For that purpose BACE measurements have been performed. The results are shown in Figure S8. Using a density of states of  $N = 10^{21} \text{ cm}^{-3}$  (the same as used in the simulations), the effective band gaps can be estimated to 1.24 eV in the devices with DIO and 1.32 eV w/o DIO which is in very good agreement to 1.29 eV or 1.39 eV as used in the simulation.

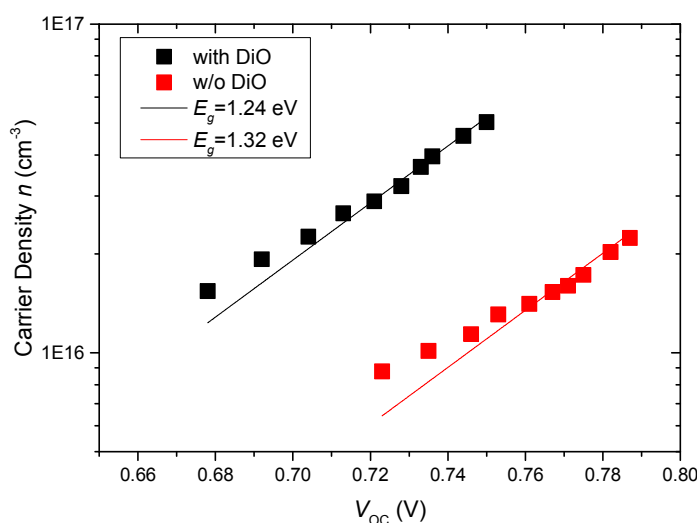


**Figure S9.** Carrier density  $n$  vs. open circuit voltage  $V_{OC}$  as determined with BACE.

In the second method, the energy level alignment of the blends on high or low work function (WF) electrodes is analyzed by Kelvin probe in the dark (ground state). If the blends are prepared on low WF aluminum, electrons are thermally injected into the unoccupied states of the blend (i.e. the PCBM LUMO). A space charge layer is formed at the contact, causing a band bending which shifts the Fermi level into the band gap (Lange et al., *Phys. Rev. Lett.* (2011), 106, 216402). The same is true if holes are injected from high WF PEDOT:PSS. However, for large distances from the electrode the band bending levels out, which is also denoted as pinning of the electrode Fermi level. Thereby, the position of the pinning levels is strongly correlated to the underlying DOS. In Figure S9 it is already obvious, that the difference between the two pinning levels in blend with DIO is reduced by 100 meV compared to the blend w/o DIO. At  $\sim 100$  nm distance from the electrode a difference of the pinning levels of 550 meV (w/o DIO) or 450 meV (with DIO), respectively, can be determined. This equals exactly the band gap reduction of 100 meV needed in the simulation.

These results also allow to estimate the effective band gap. It has been shown recently, that in the pinning regime at around 100 nm always a density of thermally injected carriers of about  $10^{15} \text{ cm}^{-3}$  is established, independent of the particular shape or broadening of the DOS (Lange et al., *J. Phys. Chem. Lett.* (2013), 4, 3865). According to the Boltzmann approximation the offset between the Fermi level  $E_F$  and e.g. the conduction band edge  $E_{CB}$  is given by

$$E_F - E_{CB} = k_B T * \ln \frac{n}{N},$$

which is 350 meV at  $T = 295 \text{ K}$ ,  $n = 10^{15} \text{ cm}^{-3}$  and  $N = 10^{21} \text{ cm}^{-3}$ . With that, the effective band gap  $E_g = E_{CB} - E_{VB}$  can be estimated to 1.25 eV in blends w/o DIO and 1.15 eV with DIO.

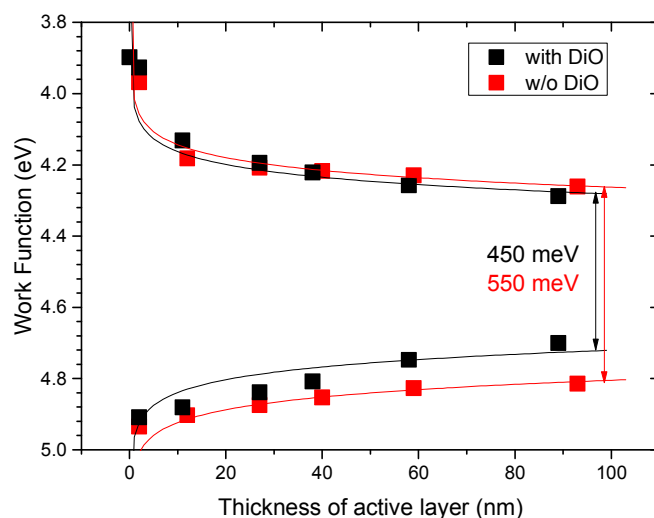


**Figure S10.** Work function (WF) evolution of the organic layer as a function of the film thickness prepared on low WF (Al) or high WF (PEDOT:PSS) electrodes as measured by Kelvin probe in the dark. The difference of the pinning levels in the blend with DIO is reduced by 100 meV compared to the blend w/o DIO.